

## Lateral Boundary Effect in Centrifuge Tests for Spudcan Penetration in Uniform Clay

Shah Neyamat Ullah<sup>1, a</sup>, Yuxia Hu<sup>2, b</sup>, David White<sup>3, c</sup> and Samuel Stanier<sup>4, d</sup>

<sup>1, 3, 4</sup> Centre for Offshore Foundation Systems, Univ. of Western Australia, Perth-6009 Australia

<sup>2</sup> School of Civil & Resource Engineering, Univ. of Western Australia, Perth-6009 Australia

<sup>a</sup>20008177@student.uwa.edu.au, <sup>b</sup>yuxia.hu@uwa.edu.au, <sup>c</sup>david.white@uwa.edu.au,

<sup>d</sup>sam.stanier@uwa.edu.au

**Keywords:** Foundation, Clay, Boundary effect, Finite element modelling.

**Abstract.** The effect of the centrifuge strongbox boundary on the penetration resistance of a spudcan foundation in uniform clay has been studied using Large Deformation FE analysis. Both smooth and rough strongbox boundaries were considered with various strongbox sizes. The spudcan penetration resistance and soil flow mechanisms were analysed. It was observed that, when the strongbox size was reduced, the spudcan penetration resistance was decreased for a smooth boundary and increased for a rough boundary. The depth of cavity formed above the spudcan during its penetration, in most cases, was determined by the soil flow around mechanism without cavity wall failure. However, cavity wall failure could be initiated when a smooth strongbox boundary was very close to the spudcan. The strongbox boundary effect on the spudcan penetration resistance can be avoided when the distance of the strongbox boundary to the spudcan centre is larger than 1.5 times of spudcan diameter for a rough boundary; or 2 times of spudcan diameter for a smooth boundary.

### Introduction

Typical jack-up structures for offshore oil and gas exploration consist of a triangular floating platform supported on retractable truss legs. The entire operational loads from the platform are transferred to the seabed via circular or polygonal foundations (commonly referred to as spudcans) with a conical underside and protruding central spigot, which improves the sliding resistance (see Fig. 1). As these foundations often penetrate very deep into the seabed (often 2 to 3D in soft uniform clay, where D is the foundation diameter), understanding of the spudcan penetration behaviour at various depths is required.

To study the spudcan penetration phenomena, extensive centrifuge testing programs were carried out at various research centres [1, 2, 3]. Specifications of the different geotechnical centrifuges around the world can be found in [4]. These centrifuge tests were conducted within strongboxes, namely the testing boxes need to be designed strong enough to withstand the elevated self-weight of the soil within. To appropriately simulate the field penetration conditions the size of the strongbox should be such that, the lateral boundary is sufficiently far away that (i) the load-penetration response measured via the load cell attached to the shaft of the foundation and (ii) the associated mechanisms are practically unaffected by the presence of the boundary.

Due to the large size of spudcan foundations (10~20m in diameter), the size of the model spudcan in centrifuge test needs to be designed carefully. With smaller model size, higher acceleration level of the centrifuge is needed to achieve its prototype size. However, in general, more stable/reliable results can be obtained with lower acceleration levels. Thus, with certain strongbox size, the maximum spudcan model size needs to be defined to avoid strongbox lateral boundary effect, and then the centrifuge acceleration level can be designed to achieve the prototype spudcan size. So far, there is no guidelines on the maximum model spudcan size that can be tested using an existing strongbox (i.e. its size is fixed).

This research is to study the strongbox lateral boundary effect on spudcan penetration resistance. Both smooth and rough strongbox boundaries were considered. Spudcan foundation penetrations in

uniform clay were simulated using Large Deformation Finite Element (LDFE) analysis incorporating the RITSS (Remeshing & Interpolation Technique with Small Strain) approach originally proposed by [5]. Strongbox sizes were varied to test the boundary effect on spudcan penetration resistance and soil flow mechanisms during penetration tests. Although the strongbox size varied with a fixed spudcan size, the results can also be applied to a fixed strongbox size with varying foundation size.

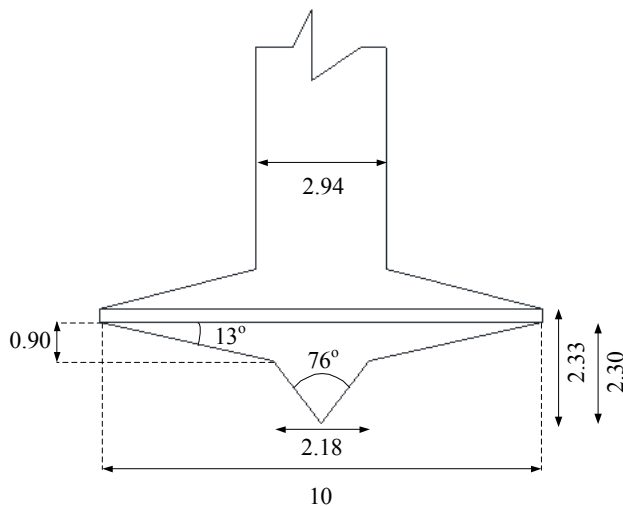


Figure 1 Spudcan dimensions in metres

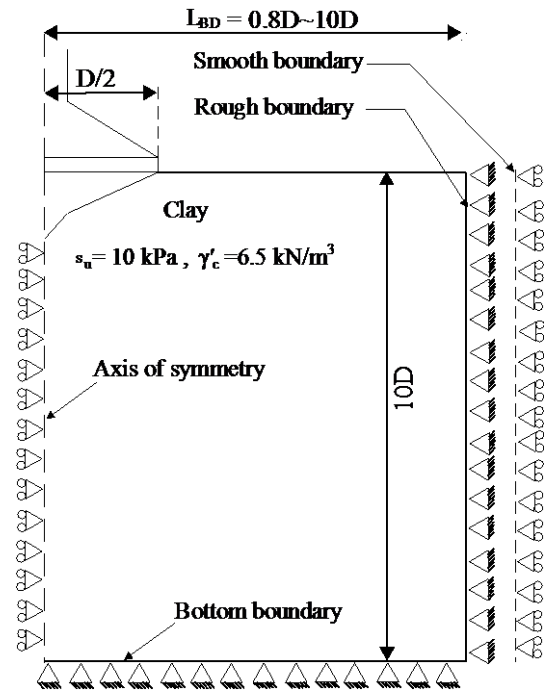


Figure 2 General problem definition

### Problem Definition

Fig. 2 depicts the general problem studied. The lateral boundary distance ( $L_{BD}$ ) is defined as the horizontal distance measured from the centre of the foundation to the inner edge of the strongbox. The  $L_{BD}$  was varied from  $0.8D$  to  $10D$  where  $D$  is the spudcan diameter. Prototype dimension of  $D = 10$  m was adopted in all the analyses as shown in Fig. 1.

Two different displacement boundary conditions have been investigated: (i) Rough boundary, where the boundary nodal displacements were restrained in the radial and vertical directions (shown as hinges in Fig. 2) and (ii) Smooth boundary, where only the radial displacements were restrained and free vertical movement of the boundary nodes was allowed (shown as roller in Fig. 2). The undrained shear strength of the uniform clay ( $s_u$ ) was 10 kPa and the effective unit weight ( $\gamma'_c$ ) was  $6.5 \text{ kN/m}^3$ . To detect the effect of the lateral boundary, all analysis results were compared to that from the simulations with  $L_{BD}$  of  $10D$ , as the result with  $L_{BD}$  of  $10D$  was a base case without boundary effect. The analysis performed beyond  $10D$  showed no practical impact on the response when compared with the  $10D$  case. Hence,  $L_{BD}=10D$  can be considered approximately equivalent to infinite soil domain conditions. Two-dimensional second order axisymmetric triangular elements were used to discretise the soil domain as in [5, 7]. The soil-spudcan foundation interface was considered rough in all analyses. Clay was simulated as fully undrained with a Poisson's ratio ( $\nu$ ) of 0.49 (essentially constant volume without the associated numerical difficulties) and stiffness ratio  $E/s_u$  of 350, which is within the typical range for soft clay [6], where  $E$  is the modulus of elasticity.

### LDfE/RITSS Approach

Significant mesh distortion would occur if conventional updated Lagrangian large deformation FE analyses were used to study large penetration problems, where soil can be excessively deformed and flow plastically around the foundation. The RITSS (Remeshing & Interpolation Technique with Small Strain) technique adopted overcomes the difficulty of mesh distortion by remeshing the complete soil domain after a certain displacement of the foundation. The previous history of the material is taken into account by linear interpolation of stress variables and material properties from the old mesh to the new mesh. Hence after each remeshing stage, the problem can be treated as a completely new problem where the distorted elements of the previous time step are replaced entirely by new undistorted elements. The method falls in the category of ALE (Arbitrary Lagrangian Eulerian) finite element methods. More details of RITSS approach can be found in [5,7]. The small strain responses for each displacement increment were calculated using the AFENA finite element program developed at the University of Sydney [8].

### Results & Discussions

The load-penetration profiles are shown in Fig. 3a and 3b for the rough and smooth boundary conditions respectively. The nominal bearing resistance ( $q_{nom}$ ) is obtained by dividing the total vertical load ( $V$ ) by the widest spudcan area ( $A=\pi D^2/4$ ). As can be seen, a rough boundary in proximity to the spudcan tends to increase the resistance whereas the smooth boundary tends to decrease it when compared with the corresponding 10D cases. The influence of the boundary is noticed from very shallow penetration depths and the influence varies with depth.

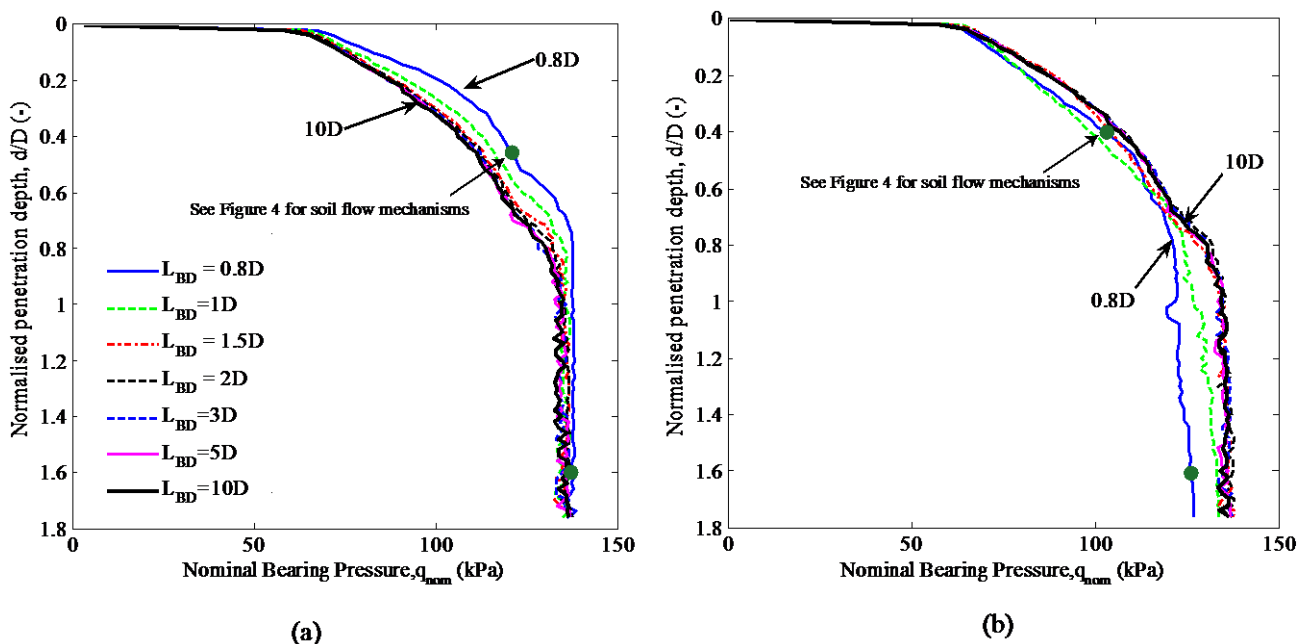


Figure 3 Load penetration response: a) rough boundary & b) smooth boundary

For the rough boundary case (Fig. 3a) comparison between the  $L_{BD}=0.8D$  and 10D reveals that, though the resistance for the former is higher, for  $d/D > 0.8$  the differences become minimal and the ultimate bearing capacity practically coincides with the 10D response. On the other hand, the smooth boundary has minimal impact on the response at shallow penetration depth for  $d/D < 0.8$ . When  $d/D > 0.8$ , the  $L_{BD} = 0.8D$  case no longer coincides with the 10D case and records a lower ultimate capacity. The deep bearing capacity factor ( $N_{cd}$ ) can be measured from the 10D case from the following expression:

$$N_{CD} = \frac{q_{nom}}{s_u} - \frac{\gamma'_c V_{spud}}{As_u} \quad (1)$$

Where,  $V_{spud}$  is the volume of the embedded spudcan including shaft. The 2<sup>nd</sup> term in Eq. 1 represents the spudcan buoyancy in clay. This result in a  $N_{cd}$  of 12.64 which is 3.5% lower than that proposed in [2] and exact plasticity solutions for a buried plate [9].

Nevertheless, the resistance curves show that a minimum  $L_{BD}$  of 2D is sufficient to avoid any effects of the boundary. This can be further reduced to 1.5D for a perfectly rough boundary (Fig.3a). It is observed in Fig. 3 that the maximum difference in spudcan penetration resistance between the  $L_{BD} = 0.8D$  and 10D is ~11% for the cases studied.

The soil flow mechanisms during spudcan penetration in uniform clay were studied by [1, 2] through centrifuge testing and complementary FE analyses such as those performed here. The overall mechanisms in these studies are broadly similar to the  $L_{BD} = 10D$  cases studied here. However, alterations to these mechanisms are evident when the boundary is placed closer to the spudcan.

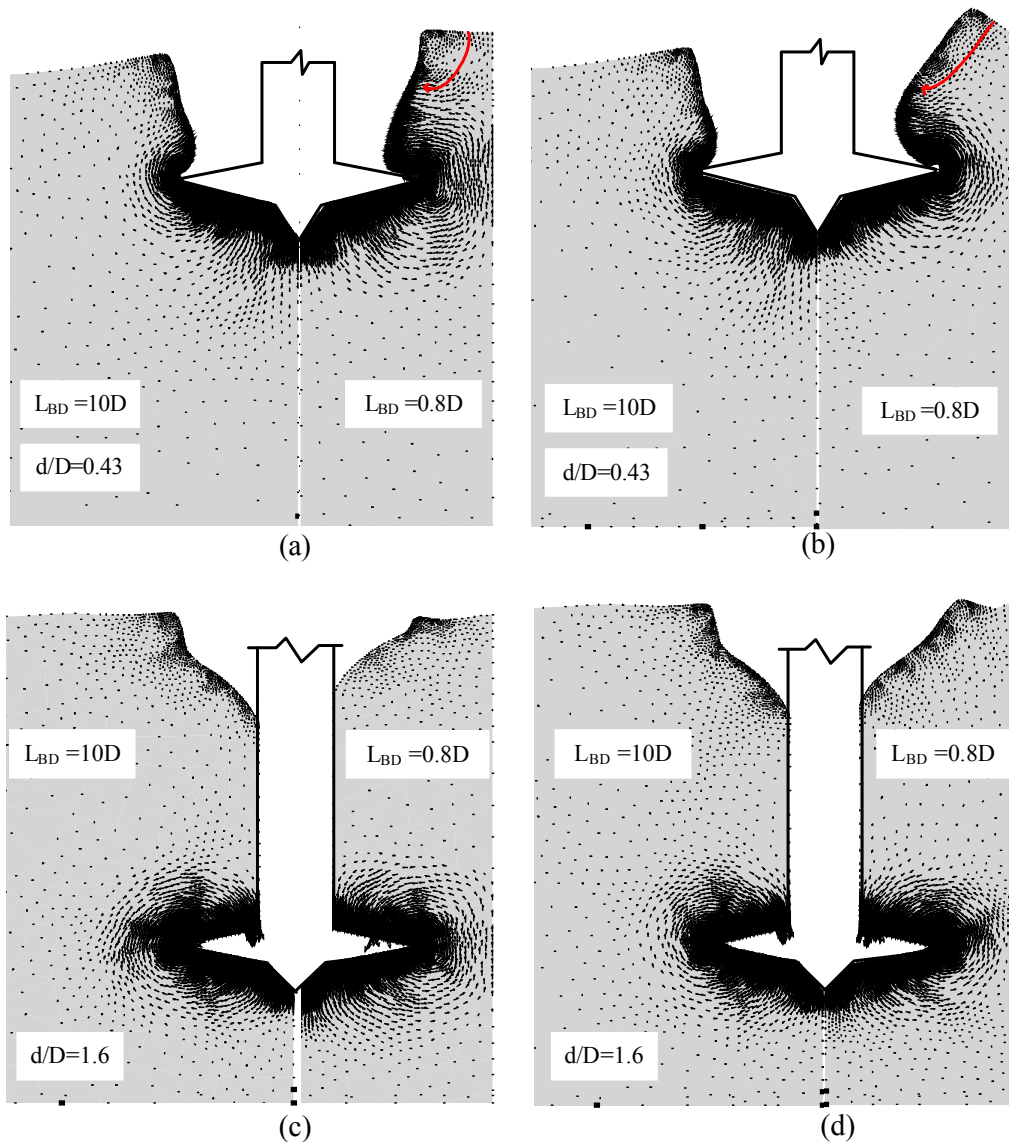


Figure 4 Effect of the lateral boundary on the soil flow mechanisms a) Smooth boundary,  $d/D=0.43$ , b) Rough boundary,  $d/D=0.43$ , c) Smooth boundary,  $d/D=1.60$  & d) Rough boundary,  $d/D=1.60$ .

To illustrate the impact of the strongbox boundary the vectorial displacement fields for  $L_{BD} = 10D$  and  $0.8D$  are compared in Fig. 4 for both rough and smooth boundary conditions at two different depth locations. Firstly, at shallow penetration of  $d/D=0.43$  (Fig. 4a & 4b) and secondly at deep penetration depth of  $d/D=1.60$  (Fig. 4c & 4d). The corresponding load penetration responses were circled in Fig. 3.

At relatively shallow penetration ( $d/D \sim 0.40$ ) for both the smooth and rough strongbox boundaries a cavity above the spudcan is observed as reported in [1]. The collapse of this cavity was shown by [1] to be caused by the soil back flow from beneath the spudcan to the exposed cavity over a wide range of parameters ( $3.5 \leq \gamma'_c D/s_u \leq 22.7$ ). However as Fig. 4a and 4b show, the conventional cavity collapse mechanism or flow type failure, where the cavity collapses due to soil flowing from beneath the spudcan to the open cavity, does not take place for the  $0.8D$  case. Rather what is observed is the reversal of soil flow direction from heave to towards the top of the spudcan with soil flowing into the exposed cavity causing it to collapse. Back flow components of soil flow are also evident simultaneously. Hence the boundary placed at  $0.8D$  causes the cavity to collapse in a combination of wall collapse and flow type mechanisms. This is understandable by the fact that a very close boundary forces excess soil to flow adjacent to the foundation edge, resulting in greater surface heave. However clay cannot rise indefinitely as the self-weight will force it to flow downwards. This combined back flow and cavity collapse mechanism were also confirmed for  $0.8D$  cases with a  $s_u \sim 17$  kPa.

With further penetration the flow is gradually localised around the spudcan with little or no surface movements (see Fig. 4c and 4d). It is noted that in Fig. 4a & 4c for the smooth boundary  $0.8D$  cases that the soil flow along the strongbox boundary is initiated throughout the penetration depth. At shallow penetration depth ( $d/D < 0.8$ ), the effects of the smooth boundary and the higher soil heave for  $L_{BD} = 0.8D$  compensate each other and the resulting resistance reduction is small (Fig. 3b). When the penetration depth is deep ( $d/D > 0.8$ ), the greater reduction of penetration resistance for  $L_{BD} = 0.8D$  is due to the mobilisation of the smooth boundary effect with localised soil flow mechanism (Fig 4c).

For the rough strongbox boundary, at shallow penetration, a large increase in penetration resistance is observed for  $L_{BD} = 0.8D$  case, since the surface heave and the closer rough boundary both contribute to the resistance. On the other hand, for deep penetration (Fig 4d) the rough boundary placed at  $0.8D$  acts as a fictitious soil interface providing confinement as though the boundary is further away. This explains the fact that during deep penetration ( $d/D > 1$ ) where the smooth boundary at  $0.8D$  lowers the resistance, while the rough boundary converges quickly and follows the  $10D$  case.

## Conclusions

The effects of the lateral boundary in centrifuge tests have been studied through Large Deformation Finite Element (LDFE) analyses using the RITSS methodology. The load penetration responses were presented for a 10 m diameter spudcan in uniform clay with undrained shear strength ( $s_u$ ) of 10kPa, whilst varying the lateral boundary distance ( $L_{BD}$  - relative to the spudcan centre) from  $0.8D$  to  $10D$ . Both rough and smooth lateral boundary conditions have been investigated. The following conclusions were reached from the study:

- A smooth lateral boundary placed in close proximity to the foundation tends to reduce the overall penetration resistance. The maximum reduction was around 9% for  $L_{BD}=0.8D$  and gradually decreased with increasing lateral boundary distances until convergence with the  $10D$  curve. On the other hand, in contrast to the smooth boundary, a rough boundary acts in increasing the penetration resistance by a maximum amount of  $\sim 11\%$  for  $L_{BD}=0.8D$ .
- A smooth boundary placed at  $0.8D$  had a consistent impact on the resistance as the failure mechanism passes through the boundary throughout the penetration depth studied. For the corresponding rough boundary case, the impact of the boundary is lowered for normalised

penetration depths ( $d/D$ ) greater unity and the deep bearing resistance for the 0.8D and 10D was almost the same.

- It was observed in all the cases studied, that although the overall resistance increase caused by a close boundary (e.g. 0.8D case) did not exceed ~11% compared to the 10D case, the cavity collapse mechanisms were different for the 0.8D cases. The cavity collapse for the 0.8D cases comprised a combination of wall failure and soil back flow failure as opposed to mainly soil back flow failure when the boundary was remote.
- To avoid the influence of the boundary on the measured penetration resistance in centrifuge tests, a lateral boundary distance of 2D measured from the centre of the foundation should be adopted if the boundary is smooth. A smaller distance of 1.5D can be used for a rough boundary.

### Acknowledgements

The work forms part of the activities of the Centre for Offshore Foundation Systems (COFS) at the University of Western Australia, which is supported by the Lloyd's Register Education Trust as a Centre of Excellence and is a node of the Australian Research Council (ARC) Centre of Excellence in Geotechnical Science and Engineering. The authors would like to acknowledge the financial contribution of the Australian Research Council (ARC) through Discovery Project No. 1096764. The third author is supported by an ARC Future Fellowship and holds the Shell Energy and Minerals Institute (EMI) Chair in Offshore Engineering.

### References

- [1] Hossain, M.S., Hu, Y., Randolph, M.F. and White, D.J., "Limiting cavity depth for spudcan foundations penetrating clay," *Geotechnique*, vol. 55, pp. 679-690, 2005.
- [2] Hossain, M.S., "New Mechanism-Based Design Approaches for Spudcan Foundations on Clay," PhD dissertation, School of Civil and Resource Engineering, University of Western Australia, Perth, 2008.
- [3] Teh, K.L., Quah, C.K., Chow, Y.K., Cassidy, M.J., Leung, C.F. and Randolph, M.F., "Revealing the bearing capacity mechanisms of a penetrating spudcan through sand overlying clay," *Géotechnique*, vol. 58, pp. 793-804, 2008.
- [4] Information on <http://www.ust.hk/~webgcf/GCFCenter.html#CCore>
- [5] Hu, Y. and Randolph, M.F., "A Practical Numerical Approach for Large Deformation Problems in Soil," *Int.J.Numer.Anal.Meth.Geomech*, vol. 22, pp. 327-350, 1998.
- [6] B. M. Das. *Geotechnical Engineering Handbook*, J.Ross Publishing, Florida, 2010.
- [7] Hu, Y. and Randolph, M.F., "H-adaptive FE analysis of elasto-plastic non-homogeneous soil with large deformation," *Computers and Geotechnics*, vol. 23, pp. 61-83, 1998.
- [8] Carter, J. P. & N. P. Balaam (2006). *AFENA users manual version 6*. Centre for Geotechnical Research, Univ of Sydney, Sydney, Australia.
- [9] Martin, C. M., and Randolph, M. F. (2001), "Applications of the lower and upper bound theorems of plasticity to collapse of circular foundations." *Proc., 10th Int. Conf. on Computer Methods and Advance Geomechanics*, Vol. 2, Tucson, Ariz., 1417–1428